IMA Journal of Applied Mathematics (2015) **80**, 494–507
doi:10.1093/imamat/hxt055
Advance Access publication on 23 January 2014

Topological attitude towards path following, applied to localization of complex dispersion characteristics for a lossy microwave, ferrite-coupled transmission line

JACEK GULGOWSKI*
Institute of Mathematics, University of Gdańsk, ul. Wita Stwosza 57, 80-952 Gdańsk, Poland
*Corresponding author: dzak@mat.ug.edu.pl

AND

JERZY JULIAN MICHALSKI
TeleMobile Electronics Ltd., Al. Zwyciestwa 96/98, 81-451 Gdynia, Poland

[Received on 23 December 2012; revised on 29 August 2013; accepted on 13 December 2013]

We are presenting a certain simplification of the well-known PL-continuation method, applied to continuous curve tracking, for zero set of the map

$$F : \mathbb{R}^{k+1} \to \mathbb{R}^k.$$

The presented algorithm builds a family of regular $(k+1)$-dimensional simplices following the set of zeros of the map F. The values of this map are calculated in the vertices of each simplex, then a decision is made as to which of the k-dimensional faces are to be taken as the faces intersected by the zero set $F^{-1}(0)$. The method is based on sign changes of coordinate functions of the map F. The computed values of F are not used in further computations. This allows for limitation of the accuracy required to calculate values of F, i.e. the calculations may be discontinued when the signs of F values may be identified. The algorithm is less restrictive than the classical PL-continuation method and its modifications like the integer labelling. As a consequence it may be observed that in many cases the algorithm is able to follow multiple branches starting from the bifurcation point. The method is applied to the solution of practical 3D problems regarding identification of complex dispersion characteristics of microwave transmission lines. While the function F is being traced, a big computational effort is required for its value at every point of the domain. Therefore every method which can accelerate this process seems to be valuable.

Keywords: path following; PL-continuation; microwave ferrite transmission line; dispersion characteristics.

1. Introduction

The problem of path (curve) following may be simply described as numerical approximation of the zero set of the continuous map $F : \mathbb{R}^{k+1} \to \mathbb{R}^k$, starting from some known zero $p_0 \in \mathbb{R}^{k+1}$. It is a natural problem in all applications related to the homotopy theory and nonlinear eigenvalue problems. For an extensive discussion on different attitudes towards this problem we can refer the reader to the monograph (Allgower & Georg, 1987) and the review paper (Allgower & Georg, 1993) by the same authors.

The methods of path following are focused on two generic ideas: predictor–corrector attitude and piecewise-linear methods, henceforth referred to as PL-continuation methods. Predictor–corrector methods may be applied in the case of a smooth map F (at least of class C^1) with a known derivative or its reasonable estimations. In contrast, PL-continuation methods do not require smoothness assumptions. In this paper we focus on the situation where a map F is of the C^1 class, but it is either not possible to find its derivative or it is very difficult to estimate. Moreover, the computational effort to calculate the value of the function F is relatively high, so it is important to limit considerably the number of points used to calculate the value of the function. That is why the predictor–corrector methods may not be applied and, instead, we are turning towards PL-continuation methods.

The first examples of PL path tracing algorithms were presented in the mid-1960s by Lemke & Howson (1964) and Lemke (1965). Let us now briefly describe this method. Later on we will refer to a convex hull of n points in $\mathbb{R}^k$ as n-simplex. If the n-simplex is a regular polytope we will call it a *regular n-simplex*. The method requires triangulation of the underlying Euclidean space $\mathbb{R}^{k+1}$—so let us assume we have such decomposition of $\mathbb{R}^{k+1}$ into $(k+1)$-dimensional simplices, that the intersection of two simplices is either empty or forms one of the lower-dimensional faces of both simplices. The triangulation induces a piecewise-linear map, i.e. the map, which is defined in each simplex belonging to the triangulation of $\mathbb{R}^{k+1}$ as an affine extension of the map F, restricted to the set of vertices of the simplex. To be precise: let us assume that σ is a $(k+1)$-dimensional simplex spanned by the vertices $v^1, v^2, \ldots, v^{k+2} \in \mathbb{R}^{k+1}$. It is also assumed we have the values of the function F calculated for all vertices v^i $(i = 1, 2, \ldots, k+2)$, and we find such a unique affine map $\tilde{F}_\sigma : \sigma \to \mathbb{R}^k$ that $\tilde{F}_\sigma(v^i) = F(v^i)$ for all $i = 1, 2, \ldots, k+2$. The union of all maps $\tilde{F}_\sigma$ is well defined on the entire domain $\mathbb{R}^{k+1}$ and forms a so-called, PL-approximation $\tilde{F}$ of the map F. The PL-continuation method is based on the simple idea: instead of following the zero set of the map F we follow the zero set of its PL-approximation $\tilde{F}$. Therefore, the curve identified by the PL continuation method is actually a polygonal curve, which is not difficult to find. In every step the algorithm identifies such k-dimensional faces σ_i of simplex σ, that there exists a zero of the map $\tilde{F}$ restricted to σ_i. This step requires solution of several $(k+1)$-dimensional linear systems. When the k-dimensional faces of simplex σ are identified, they indicate which adjacent simplices should be selected to follow the curve. Actually the algorithm selects exactly one face of the simplex (*door-in-door-out property*).

In this paper we are going to suggest that the above method may be simplified, so we will consider signs of the components $F_j(v^i)$, $j = 1, 2, \ldots, k$, $i = 1, 2, \ldots, k+2$ only. The condition selecting faces of the simplex which should be followed is less restrictive than the one used in PL-continuation methods. As a consequence, the algorithm may choose more than one face of the simplex to follow (there is no door-in-door-out property). It appears that, thanks to this additional flexibility, the algorithm may follow multiple bifurcation branches. The inspiration for the method is the 2D case, i.e. the situation when $k = 1$. This simplest case is presented below as a demonstration of the idea of the algorithm. The method was used in the paper (Michalski & Kowalczyk, 2011), and we refer readers to more technical details related to the implementation. Here we concentrate on the problems on the mathematical side and additional applications. Let us start with the precise formulation of the problem. Let us assume we have the C^1 map $F : \mathbb{R}^{k+1} \to \mathbb{R}^k$ and the set $C = F^{-1}(0)$. From the implicit function theorem we know that if $F(x_0) = 0$ and $DF(x_0)$ is of the rank k (i.e. this zero x_0 is regular), then, in the neighbourhood of the x_0, the set C is locally a C^1 curve.

Let us assume for now that all zeroes of the map F are regular, so that the set of zeroes $F^{-1}(0)$ is the union of disjoint C^1 curves. We are going to identify numerically the $C \subset F^{-1}(0)$ curve passing through the known zero $F(x_0) = 0$, $x_0 \in \mathbb{R}^{k+1}$. The procedure described here is very natural in 2D case of $F : \mathbb{R}^2 \to \mathbb{R}^1$, where the location of zeroes of F is indicated by the sign changes of this

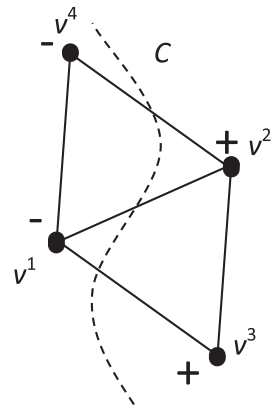

FIG. 1. Curve C crosses two faces of simplex $v^1v^2v^3$. The next simplex $v^1v^2v^4$ is built.

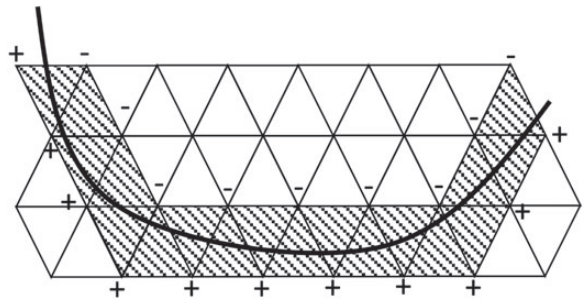

FIG. 2. Tracing of curve in $\mathbb{R}^2$.

map. A systematic and efficient attitude towards this task is described below and presented in Figs 1 and 2.

Let $F : \mathbb{R}^2 \to \mathbb{R}$ be such a continuous function and $(x_0, y_0) \in \mathbb{R}^2$ that $F(x_0, y_0) = 0$. In the first step of the algorithm we take any regular 2-simplex S with such edge of length $E > 0$ that (x_0, y_0) lies in the interior of S. Let v^1, v^2 and v^3 denote the vertices of S. We look at the signs of numbers $F(v^1)$, $F(v^2)$ and $F(v^3)$ and, in the situation where not all the numbers are of the same sign, we can easily identify the edges crossing the set of zeroes $F^{-1}(0)$.

The described situation is depicted in Fig. 1. In this case we know that the curve of solutions crosses the edges v^1v^2 and v^1v^3. We cannot say if the curve C (or any other curve) crosses the third v^2v^3 edge, but we will follow the edges with an identified sign change. In the next step of the process we will build other regular 2-simplices (having the same edge length E) and based on the edges v^1v^2 and v^1v^3, respectively. The idea is presented in Fig. 2.

As we can observe, central points of edges with an identified sign change may be considered as approximations of zeroes of the map F, and we know that each approximated zero is distanced from the actual solution by not more than $E/2$. It can be seen that the idea is very simple and we have full control over the accuracy of our approximation. The important feature of this procedure is that we can

also control computational complexity—for each simplex we calculate value of the function F at three points only, there are no gradient estimates necessary, etc. This is particularly valuable for applications where the function F requires numerous computations.

In the next section we are going to prove some lemmas in higher-dimensional cases, focusing in particular on the case of $k = 2$. Then we will describe a sample application of the algorithm for $k = 2$ and, finally, we will discuss higher-dimensional cases (i.e. for $k > 2$).

The method was first described at Michalski & Kowalczyk (2011) and applied to the search of real and complex dispersion characteristics of selected microwave guides. The idea is very natural when $k = 1$, i.e. for zeroes of the map $F : \mathbb{R}^2 \to \mathbb{R}$, but its generalization for a higher-dimensional case (in the cited paper it was actually the case of $F : \mathbb{R} \times \mathbb{C} \to \mathbb{C}$) lacked clear explanation. What is more, it was not formally proved that the method really approximates the curve of solutions. In this paper we are going to justify the suggested attitude.

2. Main results

Initially we will focus on the 3D case, i.e. the map $F : \mathbb{R}^3 \to \mathbb{R}^2$ of class C^1. Let us start with the known zero (x_0, y_0, z_0) of the map F and a regular 3-simplex surrounding this zero. Let us denote the vertices of the simplex by v^1, v^2, v^3 and v^4. In each vertex v^i $(i = 1, 2, 3, 4)$ we have a pair of real numbers $F_1(v^i)$ and $F_2(v^i)$. Similarly as in the previous section we will concentrate on sign changes of those values, but there are no such straightforward implications here as in the 2D case.

Below we will present a series of lemmas showing how we may identify which faces of simplex are intersected by the curve C of zeros of the map F. Let us first specify a necessary notation: let $\Delta \subset \mathbb{R}^2$ be a closed 2-simplex with vertices $p_1 = (0, 0)$, $p_2 = (0, 1)$ and $p_3 = (1, 0)$. We will treat this simplex as a fixed one throughout this section. For a given regular 2-simplex $\sigma \subset \mathbb{R}^3$, with vertices v^i $(i = 1, 2, 3)$, let us define such an affine map $j_\sigma : \Delta \to \sigma$ that $j_\sigma(p_i) = v^i$ for $i = 1, 2, 3$. We can actually see that j_σ is given as

$$j_\sigma(a, b) = v^1 + aw_1 + bw_2,$$

where $w_1 = v^2 - v^1$ and $w_2 = v^3 - v^2$ (so that w_1 is the vector joining v^1 with v^2 and w_2 is the vector joining v^2 and v^3).

Let us define a map $g_\sigma : \Delta \to \mathbb{R}^2$ by $g_\sigma(x, y) = F(j_\sigma(x, y))$. We will apply the topological degree (Brouwer degree) concept (cf. Krawcewicz & Wu, 1997; Nirenberg, 1974)

Lemma 1 Let us assume that we have such a regular 2-simplex $\sigma \subset \mathbb{R}^3$ with vertices v^1, v^2, v^3 and edge length $E > 0$ that $\sigma \cap F^{-1}(0) = \{(x_1, y_1, z_1)\}$. Let us also assume $(x_1, y_1, z_1) \in j_\sigma(\mathrm{Int}\Delta)$ that the following conditions are satisfied:

(A1) $DF(x_1, y_1, z_1)$ is of the rank 2, so the set $F^{-1}(0)$ is locally described by a curve $\gamma : (-\delta, \delta) \to \mathbb{R}^3$, where $\gamma(0) = (x_1, y_1, z_1)$;

(A2) the vectors $\gamma'(0)$, $w_1 = v^2 - v^1$ and $w_2 = v^3 - v^2$ are linearly independent (it may be interpreted as curve γ passing through the simplex σ)

Then $\deg(g_\sigma, \Delta, 0) \neq 0$.

Proof. Because the map g_σ has only one zero $(a_0, b_0) = j_\sigma^{-1}(x_1, y_1, z_1)$ in the set Δ, which does not belong to the boundary $\partial\Delta$, and the map g_σ is clearly the C^1 map, it is sufficient to show that $Dg_\sigma(a_0, b_0)$ is a linear isomorphism.

We can see that $Dg_\sigma(a_0, b_0) = DF(x_1, y_1, z_1) \circ Dj_\sigma(q_0)$ and $Dj_\sigma(a_0, b_0) = [w_1, w_2]$. As $DF(x_1, y_1, z_1)$ is of rank 2, we can see that the 1D kernel of this linear map is spanned by the vector $\gamma'(0)$. Hence, if $Dg_\sigma(a_0, b_0)(\bar{q}) = 0$ for some $\bar{q} = (\bar{a}, \bar{b}) \in \mathbb{R}^2$, then $j_\sigma(\bar{q}) = \bar{c}\gamma'(0)$ for some real constant $\bar{c}$. Then there is $\bar{a}w_1 + \bar{b}w_2 = \bar{c}\gamma'(0)$, which is possible only when $\bar{a} = \bar{b} = \bar{c} = 0$. Therefore, the differential $Dg_\sigma(a_0, b_0)$ is an isomorphism, which completes the proof. □

REMARK 2.1 The lemma may be applied to the faces of 3-simplex as discussed below. However, we have to remember that assumptions (A1) and (A2) refer to the properties of the set of zeros $F^{-1}(0)$ in the faces of the 3-simplex only. It does not matter what happens in the simplex interior—the lemma, in particular, remains valid if there is a bifurcation point inside the simplex. Assume now that we have four branches that emanate from the bifurcation point (i.e. we have the point where two curves intersect) and each of the branches intersects (transversally) different face of the 3-simplex. In this case for each face σ the map g_σ has non-zero Brouwer degree.

This simple observation leads to the general idea of the algorithm: out of all the faces of the 3-simplex we must either choose the ones which show a non-zero degree of the map g_σ or reject the faces when we know that the degree of the map g_σ equals zero. The next lemma helps us to identify the faces which should be rejected.

LEMMA 2 Let us assume we have such a regular 2-simplex $\sigma \subset \mathbb{R}^3$, with vertices v^1, v^2, v^3 and edge length $E > 0$, that for some $j = 1, 2$
(B1) $F_j|_{\partial\Delta} \neq 0$, i.e. the function F_j has a constant sign for all the points c in the boundary of the simplex σ.

Then $\deg(g_\sigma, \Delta, 0) = 0$.

Proof. It can be observed that the map F_j satisfying (B1) does not achieve 0 on the 1D faces of the simplex σ. This means that one of the following holds true:

$$g_\sigma(\partial\Delta) \subset (0, +\infty) \times \mathbb{R},$$
$$g_\sigma(\partial\Delta) \subset (-\infty, 0) \times \mathbb{R},$$
$$g_\sigma(\partial\Delta) \subset \mathbb{R} \times (0, +\infty),$$
$$g_\sigma(\partial\Delta) \subset \mathbb{R} \times (-\infty, 0).$$

In either of these situations the map $g_\sigma|_{\partial\Delta}$ may be extended to the map $\bar{g}_\sigma : \Delta \to \mathbb{R}^2$, which does not attain a zero. Therefore, we can see that the map g_σ may be joined by homotopy with such a map $\bar{g}_\sigma$ that $\bar{g}_\sigma(a, b) \neq 0$ for all $(a, b) \in \Delta$, hence $\deg(g_\sigma, \Delta, 0) = 0$. □

The two lemmas given above lead to the following conclusion:

COROLLARY 1 Let us assume that we have a regular 3-simplex σ surrounding zero of the map F, and that there exists a curve of solutions γ intersecting two faces of the simplex σ so that the conditions (A1) and (A2) are satisfied. Additionally we assume that the two faces of the simplex σ satisfying the condition (B1) can be identified. Then the remaining two faces are crossed by the curve γ.

As we can see, the condition (B1) may be difficult to verify. Later we are going to present certain approximations of this condition, which may be practically applied. However, before we continue, let us observe that the corollary specified above may be turned into the path following the algorithm, which

is very close to the PL-continuation method. Henceforth we will refer to this algorithm later as a 'follow sign changes' (FSCs) algorithm.

1. The algorithm starts from the initial zero of the map F and the initial 3-simplex σ_0 surrounding this zero.
2. For a given simplex σ_i we identify its 2D faces, satisfying the condition (B1). These faces will be excluded from further processing.
3. For each 2D face of σ_i, which was not discarded in the previous step, the pivoting step is performed and the regular 3-simplex σ_i' different then σ_i is found. Then it is checked if σ_i' was processed before. If not, then σ_i' is placed into stack for further processing.
4. Take the next 3D simplex from the stack and return to step 2.
5. The algorithm requires some boundary stop condition, e.g. we exclude all the faces which contain at least one vertex outside of the predefined cube.

REMARK 2.2 The centre of each 3-simplex placed on the stack is considered to be the approximation of the zero of F.

In the practical implementation of the step 3 we need to build the list L of all processed simplices. And we face two problems: the first one is the growth of the list L and the stack, and the second one is the way to check if the 3-simplex is in the list L or not. The two problems are related because the more simplices we process the more time is needed to check whether the next one was processed or not. In order to simplify the calculations we assume that the simplex was processed before if its centre is distanced from the centre of one of simplices in the list L less then $2r(E)$, where $r(E)$ is the radius of the $(k+1)$-dimensional sphere inscribed in the regular simplex with the edge length E. When the list L grows, the time needed to review all its elements becomes too long and then it is worth to index the elements in the list L to speed up the searching process—e.g. indexing each coordinate separately.

Let us now briefly compare FSC algorithm to the PL-continuation method described in the Introduction. First of all, we should observe that both FSC and PL-continuation methods offer similar computational performance as far as the number of evaluations of the function F is concerned. Now let us refer to Fig. 3, where the sample location of values $F(v^i)$ is presented.

As we can see, the method based on sign changes on the boundary of the simplex σ is less restrictive then the PL-continuation method. It will follow the faces which have the range like $F(\sigma)$ in Fig. 3, while the PL-continuation method will not continue along such faces. Therefore, we can expect that the method of sign changes will generate larger sets approximating $F^{-1}(0)$ then those generated by the PL-continuation method. The good side was mentioned in Remark 2.1: the FSC algorithm may follow all branches emanating from the bifurcation point (as opposed to door-in-door-out property of the classical PL-continuation method). But it may also happen that additional, *spurious*, solutions may appear.

Let us observe that the only situation, where the difference between the two methods may generate the spurious solutions is when both components F_1 and F_2 of the map F show the sign change on the boundary of σ, but the affine extension of F from the vertices does not have a zero in σ. Let us discuss the consequences of this decision in case of the FSC algorithm.

We can observe that in the case when F is the C^1 map and the surfaces $F_1^{-1}(0)$ and $F_2^{-1}(0)$ are intersecting transversally, spurious solutions are a local phenomenon, and may not appear far away from the curve of solutions. In other words: if we turn into the wrong face, we will have to stop when we leave the neighbourhood of the set $F^{-1}(0)$. The effect depends on the geometry of the surfaces and the size

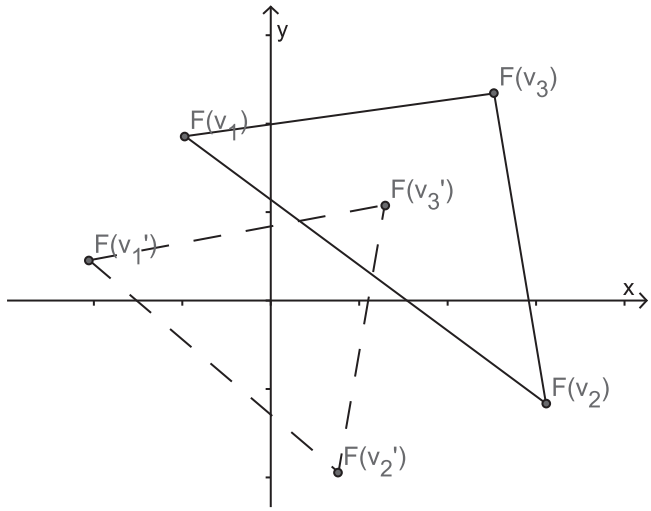

FIG. 3. Two positions of the range $F(\sigma)$ and $F(\sigma')$ showing the same sign changes, which indicates that there may exist a zero both in σ and σ'. The PL-continuation method indicates the zero for σ' but not for σ. $F(\sigma)$ is presented with a solid line, $F(\sigma')$ with a dashed line.

of the simplex E, but for the given C^1 map F we can always find E which is small enough, so that the spurious solutions will disappear after several steps (the number of steps may be estimated). This effect may be observed in practice: the curve is sometimes 'thicker' than a single simplex. The geometrical explanation of this fact will follow. We may treat it also as a short discussion on the accuracy of the algorithm.

Let us assume that there is a zero set given as the intersection of the two surfaces $F_1^{-1}(0)$ and $F_2^{-1}(0)$, where $F_i : \mathbb{R}^3 \to \mathbb{R}^1$ are C^1 maps. Let us define the open E-neighbourhood of the set $A \subset \mathbb{R}^3$ as

$$N_E(A) = \{p \in \mathbb{R}^3 \mid \operatorname{dist}(p, A) < E\},$$

where $\operatorname{dist}(p, A) = \inf\{|a - p| : a \in A\}$. In this case we can see that, for the simplex edge length E, the traced curve will be contained in the set

$$\overline{N_E(F_1^{-1}(0))} \cap \overline{N_E(F_2^{-1}(0))}.$$

Let us assume that, contrary to our claim, we have a regular 3-simplex σ and one of its vertices v is such that $v \notin N_E(F_i^{-1}(0))$ for some $i \in \{1, 2\}$. Then $\operatorname{dist}(v, F_i^{-1}(0)) > E$, which implies that no point of the simplex intersects the zero set of the function F_i, so the function F_i has a constant sign in the entire simplex σ. This means that all the faces of such simplex would be discarded by the FSC algorithm, so the algorithm would never leave the set

$$\overline{N_E(F_1^{-1}(0))} \cap \overline{N_E(F_2^{-1}(0))}.$$

Knowing the values

$$\varepsilon_i(E) = \sup\{|F_i(p)| : F_i(q) = 0 \wedge |p - q| \leqslant E\},$$

which are actually the modulus of continuity of functions F_i in zeroes of F_i, we can say that all solutions p given by the FSC algorithm satisfy $|F_i(p)| \leqslant \varepsilon_i(E)$. Particularly, if F_i is a Lipschitz continuous with constant L, we can say that for all FSC solutions p we have $|F_i(p)| \leqslant LE$.

Now let us proceed to practical approximations of the condition (B1).

LEMMA 3 Let us assume that we have a regular 2-simplex $A \subset \mathbb{R}^3$ with vertices v^1, v^2, v^3 and edge length $E > 0$, and that for some $j = 1, 2$ the following conditions (C1) and (C2) are satisfied:

(C1) all values $F_j(v^i)$ $(i = 1, 2, 3)$ have the same sign;

(C2) for each $c \in [v^n, v^m]$, where $n, m = 1, 2, 3$, $i \neq j$ we have $\langle \nabla F_j(c), w \rangle \neq 0$, where $w = v^m - v^n$ is the vector joining v^n with v^m and $[v^n, v^m]$ is the edge joining vertices v^n and v^m.

In such a situation the condition (B1) is satisfied as well.

Proof. Let us start with the observation that the conditions (C1) and (C2) constitute a guarantee that the map F_j does not achieve 0 on the 1D faces of the simplex A. Let us take any edge $[v^n, v^m]$ and consider the map $\varphi : [0, 1] \to \mathbb{R}$ given by

$$\varphi(t) = F_j((1 - t)v^n + tv^m) = F_j(v^n + tw).$$

The map φ attains the same values as F_j on the edge $[v^n, v^m]$. We can also observe that $\varphi'(t) = \langle \nabla F_j(v^n + tw), w \rangle$ is of a constant sign, and so we know that φ is a monotone. Moreover, since $\varphi(0)$ and $\varphi(1)$ have the same sign, we can conclude that $\varphi([0, 1]) \in (0, +\infty)$ or $\varphi([0, 1]) \in (-\infty, 0)$. □

REMARK 2.3 We should note that in order to check the condition (C2) we need to know the derivative of the map F. In this case it is usually much more efficient to use the predictor-corrector methods. On the other hand, the condition (C2) may also appear to be difficult to check. In our simulations we will use more practical conditions. First of all, if we know the exact form of ∇F_j, we may use the following approximation:

(C2′) the values $\langle \nabla F_j(v^n), w \rangle$ and $\langle \nabla F_j(v^m), w \rangle$ should have the same sign.

On the other hand, if we do not have the direct form of the gradient ∇F_j, we may look at a certain approximation of the value $\langle \nabla F_j(v), w \rangle$, which is actually the directional derivative of function F_j along a vector w at point v. Hence we may approximate this value by a quotient $(F_j(\alpha) - F_j(\beta))/(\alpha - \beta)$ for appropriately selected values of α and β, and replace (C2) with

(C2″) the differences $F_j(v^n) - F_j(\bar{v})$ and $F_j(\bar{v}) - F_j(v^m)$ are of the same sign, where $\bar{v} = \frac{1}{2}(v^n + v^m)$.

Depending on the function F_j some other modifications of condition (C2) may be used.

We can also ask whether it is enough to take into consideration only condition (C1) (as it is used in Michalski & Kowalczyk, 2011). When we replace condition (B1) with (C1), it will be less restrictive. Consequently, we will exclude more simplex faces with condition (C1) than with condition (B1). With condition (C1) it may happen that we will receive the subset of the $F^{-1}(0)$ and not follow all of its branches.

We should now refer to the integer labelling method, which is also based on sign changes of the coordinate functions in simplex vertices. This method is specified in paper (Allgower & Schmidt, 1985) and assumes identification of *completely labelled simplices* which yield 'nearly zero points' of the map F. In the 3D case the label of the vertex v is the integer number from the set $\{0, 1, 2\}$, which is equal to the number of leading non-negative components of $F(v)$. The simplex is completely labelled when the labels of its vertices cover the entire set $\{0, 1, 2\}$. As we can see, the condition (C1) is not satisfied

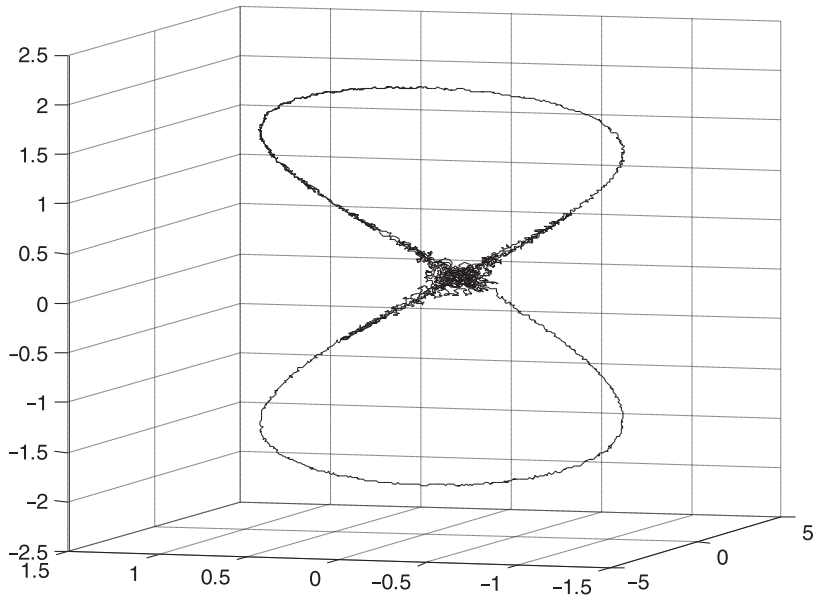

FIG. 4. Viviani's curve recreated with FSC algorithm with conditions (C1) and (C2′).

by each completely labelled simplex. On the other hand, simplexes which do not satisfy (C1) are not necessarily completely labelled. We can take the simplex where the signs of $F(v^1)$, $F(v^2)$ and $F(v^3)$ are given as $(-,-)$, $(+,+)$ and $(+,+)$ as an example. In this case the labels of the vertices are 0, 2 and 2. Therefore the rule 'select faces that do not satisfy (C1)' is less restrictive then 'select completely labelled faces'.

EXAMPLE 2.1 Let us trace the Viviani's curve given by

$$F(x,y,z) = (x^2+y^2+z^2-4, (x-1)^2+y^2-1).$$

The zero set is a closed curve with singularity in $(2,0,0)$ (in the neighbourhood of this point the zero set is not homeomorphic to a segment). The tracing algorithm was started from the point $(0,0,2)$. The simplex edge $E = 0.028$ was selected. The calculations were performed in the cube $[-3,3]^3$.

The result of the tracing algorithm is presented in Fig. 4. We needed 12,412 iterations to draw this curve. The interesting observation is that the result of the FSC algorithm is nearly the same with (C1) condition for face rejection. In this simpler case we have 12,055 iterations, so in 357 cases condition (C1) was satisfied and (C2′) was not, while the face was not rejected.

Let us also estimate the maximal 'thickness' of the traced curve in this case. The E-neighbourhood of Viviani's curve is contained in the intersection of E-neighbourhoods of the two surfaces, i.e.

$$U = \{(x,y,z) \in \mathbb{R}^3 : 2 - E < \sqrt{x^2+y^2+z^2} < 2 + E\}$$
$$\cap \{(x,y,z) \in \mathbb{R}^3 : 1 - E < \sqrt{(x-1)^2+y^2} < 1 + E\}$$

for any edge length $E \in (0,1)$.

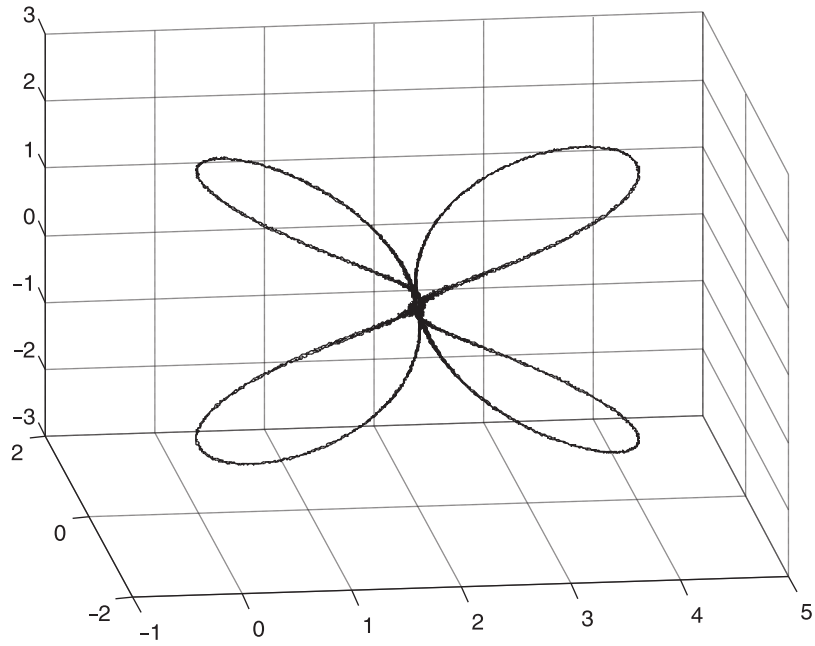

FIG. 5. Doubled Viviani's curve recreated with FSC algorithm with condition (C1) only.

The previous example shows that the bifurcation point in the solution curve is identified and all branches emanating from this point are traced.

Let us check how this works when there is even more solution branches starting from the bifurcation point.

EXAMPLE 2.2 Let us trace the solution set being 'doubled' Viviani's curve given by

$$F(x,y,z) = ((x^2+y^2+z^2-4)((x-4)^2+y^2+z^2-4), ((x-1)^2+y^2-1)((x-3)^2+y^2-1)).$$

As before, the point $(2,0,0)$ is the bifurcation point, but there are eight solution branches in the neighbourhood of this point (Fig. 5).

As we can see the algorithm identifies the solution set correctly.

3. Complex dispersion characteristics of selected microwave guides

We are going to apply the procedure described in the previous section to the process of searching for zeros of the complex valued map $F : \mathbb{R} \times \mathbb{C} \to \mathbb{C}$ which describes complex dispersion characteristics of certain microwave transmission lines. The line considered is the ferrite coupled line presented in Fig. 6.

The method used in present calculations is based on the spectral domain method. For details we refer the readers to the papers by Itoh & Mittra (1973, 1974) describing the method (see also later applications of Mazur *et al.*, 2002; Michalski *et al.*, 2002; Rosa *et al.*, 2003).

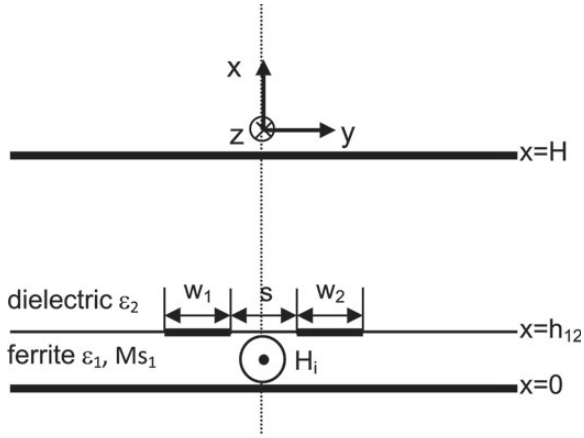

FIG. 6. Cross-section of a slab dielectric waveguide of microstrip-slotted ferrite coupled line.

For the considered line the dispersion characteristic is given by

$$\det M(f, \alpha + \mathrm{i}\beta) = 0,$$

where f corresponds to the wave frequency, while $\alpha + \mathrm{i}\beta$ is a complex propagation coefficient. In order to build the matrix M the currents on microstrips are represented by their Fourier transforms truncated to five initial components relative to some basis, and put into relations in accordance with the spectral domain method (see Itoh & Mittra, 1973, 1974). The above-mentioned relations arise from the continuity principle of electric and magnetic fields.

The dimension of the matrix M depends on the number of series elements of tangent currents J, on the strip w. The elements of the matrix M are defined as integrals and, in this case, evaluation of the function takes a relatively long time.

Let us consider the map $F : \mathbb{R}^3 \to \mathbb{R}^2$ given by $F(f, \alpha, \beta) = \det M(f, \alpha + \mathrm{i}\beta)$, where complex value of the determinant is treated as a 2D vector, i.e. an element of $\mathbb{R}^2$.

We are using the simplest version of the FSC algorithm with condition (C1) for face rejection. The simplex edge length is $E = 0.06$. The following values were used in our simulation (in *mm*): $s = 0.5$,$w_1 = w_2 = 0.6$, $h_{12} = 0.635$ and $H = 3.0$. The result is presented in Fig. 7. Physical properties of the materials are described by constants $\varepsilon_1 = 15$, $Ms_1 = 141$ kA/m, $Hi = 0$ and $\varepsilon_2 = 1$.

We assumed the ferrite with losses. This effect was simulated by the assumption that the coefficient μ_a in the Polder tensor is given by

$$\mu_a = \frac{\gamma(M_s + \mathrm{i}\Delta H)}{f},$$

where $\Delta H = 4$ kA/m. In the above formula M_s is a ferrite magnetization saturation, γ is a ferrite gyromagnetic ratio and f is the electromagnetic wave frequency.

Let us recall that the Polder tensor is given by

$$\begin{bmatrix} \mu & -\mathrm{i}\mu_a & 0 \\ \mathrm{i}\mu_a & \mu & 0 \\ 0 & 0 & 1 \end{bmatrix}.$$

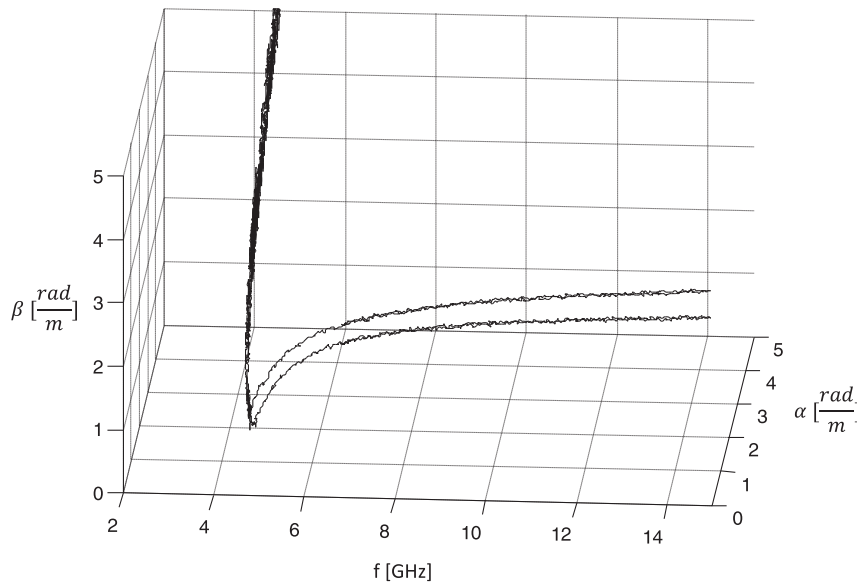

FIG. 7. Dispersion characteristics $F(f, \alpha, \beta) = 0$ of microstrip slotted ferrite and dielectric lines.

While analysing the obtained dispersion characteristics we can see two modes propagating above a cut-off frequency at $f = 4.5$ GHz. Below this frequency the value α is relatively high and the waves cannot propagate.

4. Higher-dimensional cases

In this section we will present possible generalization of the algorithm to higher-dimensional cases of the map $F : \mathbb{R}^{k+1} \to \mathbb{R}^k$. Let us now assume that the regular $(k+1)$-simplex σ is given and we have $k+2$ vertices $v^1, v^2, \ldots, v^k, v^{k+1}, v^{k+2}$. For each vertex v^i the value $F(v^i) \in \mathbb{R}^k$ is taken and we are interested in signs of all the coordinates $F_j(v^i)$. As we generalize the ideas described in Section 2, we expect that we should follow the algorithm:

(1) take all the k-dimensional faces σ_i of simplex σ (here the face σ_i is the one which does not contain vertex v^i) and verify which of them may be excluded from further processing;

(2) the face σ_i should be excluded from further processing if the higher-dimensional version of the condition (B1) is satisfied, i.e. when we know that there exists a map F_j which has a constant sign when restricted to the boundary of σ_i;

(3) we follow all the faces which were not rejected—for each such face we build the next regular $(k+1)$-simplex by finding a vertex $\bar{v}^i$ opposite to σ_i, but different from v^i.

Before we present modifications of Lemmas 1 and 2, we need to update the notation used. Now $\Delta \subset \mathbb{R}^k$ is a k-simplex spanned by vertices $p_1 = 0$, $p_{i+1} = e_i$ for $i = 1, 2, \ldots, k$ where e_i is the ith standard basis vector in $\mathbb{R}^k$. Similarly as before, for the k-simplex $\sigma \subset \mathbb{R}^{k+1}$ let us define $j_\sigma : \Delta \to \sigma$ as an

affine map mapping $j_\sigma(p_i) = v^i$ for $i = 1, 2, \ldots, k$. The proofs of these lemmas are omitted as simple generalizations of Lemmas 1 and 2.

LEMMA 4 Let us assume that we have such a regular k-simplex $\sigma \subset \mathbb{R}^{k+1}$ with vertices v^i $(i = 1, 2, \ldots, k+1)$ and edge length $E > 0$ that $\sigma \cap F^{-1}(0) = \{q_0\}$. Also, we assume that $q_0 \in j_\sigma(\mathrm{Int}\Delta)$ and the following conditions are satisfied:

(D1) $DF(q_0)$ is of the rank k, so the set $F^{-1}(0)$ is locally described by such a curve $\gamma : (-\delta, \delta) \to \mathbb{R}^{k+1}$ that $\gamma(0) = q_0$;

(D2) the vectors $\gamma'(0)$, $w_i = v^i - v^1$ where $i = 2, 3, \ldots, k+1$ are linearly independent (it may be interpreted that the curve γ passes through the simplex σ)

Then $\deg(g_\sigma, \Delta, 0) \neq 0$.

LEMMA 5 Let us assume that we have such a regular k-simplex $\sigma \subset \mathbb{R}^{k+1}$ with vertices v^i $(i = 1, 2, \ldots, k, k+1)$ and edge length $E > 0$ that for some $j = 1, 2, \ldots, k$

(D1) all the values $F_j(c)$ for $c \in j_\sigma(\partial\Delta)$ have the same sign.

Then $\deg(g_A, \Delta, 0) = 0$.

5. Conclusions

The suggested FSC algorithm follows the general philosophy of the PL-continuation method but allows for decrease in its computational costs. This is not even the question of solving the system of linear equations required by the PL-continuation method but, with the FSC philosophy, we may save a lot of time when calculating of values of the function F, since we do not have to calculate these values with a given precision but rather decide what the sign of this value is. This benefit of the algorithm is less important (or even not observed) when the values of F will be close to 0, but when we move away from zeroes of F, then it is easier to decide when the calculations should be stopped.

The presented algorithm requires no special treatment of bifurcation points appearing on the traced curve of zeroes of the map F but simply follows the identified branches, which are crossing the faces of the regular simplex in the neighbourhood of the bifurcation point.

At best, the accuracy of the method is determined by the length of the edge E of the simplex, but spurious solution branches responsible for the 'thickness' of the identified branch may appear. The influence of this effect on the algorithm accuracy has been discussed above.

Acknowledgement

We thank the referees for the comments that helped us to improve this paper.

REFERENCES

ALLGOWER, E. L. & GEORG, K. (1987) *Introduction to Numerical Continuation Methods*. Philadelphia, PA: Society for Industrial and Applied Mathematics.

ALLGOWER, E. L. & GEORG, K. (1993) Continuation and path following. *Acta Numerica*, **2**, 1–64.

ALLGOWER, E. L. & SCHMIDT, P. H. (1985) An algorithm for piecewise-linear approximation of an implicitly defined manifold. *SIAM J. Numer. Analysis*, **22**, 322–346.

ITOH, T. & MITTRA, R. (1973) Spectral-domain approach for calculating the dispersion characteristic of microstrip lines. *IEEE Trans.*, **MTT-21**, 496–499.

ITOH, T. & MITTRA, R. (1974) A technique for computing dispersion characteristics of shielded microstrip lines. *IEEE Trans.*, **MTT-22**, 896–898.

KRAWCEWICZ, W. & WU, J. (1997) *Theory of Degrees, With Applications to Bifurcations and Differential Equations*. New York: Wiley-Interscience.

LEMKE, C. E. (1965) Bimatrix equilibrium points and mathematical programming. *Manage. Sci.* **11**, 681–689.

LEMKE, C. E. & HOWSON, J. T. (1964) Equilibrium points of bimatrix games. *SIAM J. Appl. Math.*, **12**, 413–423.

MAZUR, J., MAZUR, M. & MICHALSKI, J. (2002) Coupled-mode design of ferrite-loaded coupled-microstrip-lines section. *Microw. Theory Techn.*, **50**, 1487–1494.

MICHALSKI, J. J., & KOWALCZYK, P. (2011) Efficient and systematic solution of real and complex eigenvalue problems employing simplex chain vertices searching procedure. *Microw. Theory Techn.*, **59**, 2197–2205.

MICHALSKI, J., MAZUR, M. & MAZUR, J. (2002) Scattering in a section of ferritecoupled microstrip lines: theory and application in nonreciprocal devices. *Proc. Inst. Elect. Eng. Microw., Antennas, Propag.*, **149**, 286–290.

NIRENBERG, L. (1974) *Topics in Nonlinear Functional Analysis.* New York: Courant Institute of Mathematical Sciences, New York University.

ROSA, M., ALBUQUERQUE, M. L., D'ASSUNCAO, A. G. & GIAROLA, A. J. (1993) Spectral domain analysis of coupled microstrip lines on magnetized ferrite substrates. *Int. J. Infrared Millimeter Waves*, **14**, 1531–1545.